

COASTAL WETLAND MAPPING USING TIME SERIES SAR IMAGERY AND LIDAR: ALLIGATOR RIVER NATIONAL WILDLIFE REFUGE, NORTH CAROLINA

Thomas Allen, Associate Professor

Yong Wang, Professor

Brent Gore, M.A. Candidate

Department of Geography

East Carolina University

Greenville, NC 27858

allenth@ecu.edu

wangy@ecu.edu

goreb10@students.ecu.edu

John Swords, SE Wetlands Coordinator

U.S. Fish and Wildlife Service

300 Westgate Center Drive

Hadley, MA 01035

John_Swords@fws.gov

Doug Newcomb, Cartographer

U.S. Fish and Wildlife Service

Raleigh, NC 27636-3726

Doug_Newcomb@fws.gov

ABSTRACT

Mapping and monitoring of vast coastal wetlands vulnerable to dynamic coastal erosion, sea-level rise, fire, and marsh succession require remote sensing approaches that capitalize on newly available sensors, advanced classification techniques, and combinations of multi-sensor and multi-date data. This pilot study assesses the feasibility and accuracy potential for mapping specific coastal wetlands of high priority for the National Wetland Inventory (NWI) in the Alligator River National Wildlife Refuge, North Carolina. Wetland classes of high mapping value owing to their ecological dynamics and extent include palustrine forests (swamp forests and pocosins), emergent estuarine marshes, irregularly-flooded shrub-scrub transition, and invasive *Phragmites australis* patches occurring along shores throughout the region. These classes selected to test input data and classification methodology using an array of multirate SAR imagery (ALOS PALSAR) and LiDAR-derived rasters (minimum elevation, vegetation canopy height, slope, and curvature) in combinations. Initial results illustrate strong potential for multirate SAR imagery and enhanced accuracy achievable by integration of vegetation canopy LiDAR for broad-scale mapping of coastal wetland vegetation change. Canopy structural changes over spring, early and late summer seasons were captured by PALSAR HH and HV polarization bands, yielding the highest overall accuracies multirate combination and with inclusion of LiDAR canopy and minimum elevation data. Field observations corroborated the remote sensing and offer useful calibration data for sea-level rise simulation models and invasive species monitoring. In concert with the historical continuity of Landsat for broader coastal land cover dynamics, these data and techniques offer significant enhancements for future monitoring of coastal change.

KEYWORDS: Synthetic Aperture Radar, LiDAR, wetlands, National Wetland Inventory

INTRODUCTION

Background

Wetlands have attracted strong attention by the remote sensing community owing to their high priority for natural resource management and challenges associated with their inventory, change, and provision of timely and accurate geospatial information. Coastal wetlands are vital barometers of climate change in their sensitivity to sea-

level rise, role in the global carbon cycle, and their provision of biodiversity and buffers, both in terms of nutrient cycles in estuaries and abatement of storm surges and coastal erosion. Difficulties arising in regional inventory and synoptic coverage of wetlands, however, are imposing. In particular, very high thematic and spatial resolution are frequently sought, such as for environmental impact or ecological management, and regional and national programs for monitoring wetlands have tended to restrict their map production to traditional aerial photointerpretation, such as the US Fish and Wildlife Service's National Wetland Inventory (NWI.) In addition to capturing species-related vegetation associations and zonation, several authors have noted the fundamental hydrologic dynamics of wetlands compound these problems, inducing corresponding temporal complexity to their optical signatures and sub-canopy structure (e.g., Kasischke and Borgeau-Chavez 1997.) Multidate and multi-source data are thus increasingly sought to disentangle these sources of possible confusion to mapping and inventorying programs using remote sensing, especially where areas of study are vast or inaccessible. Such problem-reducing approaches may include hydrology in the classification product, such as hydrogeomorphic classification (Hamilton et al., 2007) or the use of image classification techniques such as spectral unmixing to discern fractional composition of wetlands (e.g., Rogers and Kearney, 2004.) Geospatial analysis and hydrologic simulation modeling may also be adapted to provide complementary input data for classification, such as the use of floodplain inundation models (Townsend and Walsh, 1998) and has a history of success at improving forest classification in complex topographic environments (c.f., Franklin 1991.)

The emerging capabilities of an array of Synthetic Aperture Radar (SAR) and Light Detection and Ranging (LiDAR) sensors has attracted research expanding the possibilities to further overcome difficulties of coastal mapping and change detection. ERS-1 SAR imagery has provided a successful means to map hydrologic associations of vegetation in the Everglades and to monitor changes in hydroperiod over a regional scale (Borgeau-Chavez and Kasischke 2005.) New sensors and application of noise and speckle-suppression image filtering techniques have also met with successes for coastal wetland mapping. For example, Kushwaha et al. (2000) evaluated several filters for noise reduction to time series ERS-1 SAR data. Intensity-hue-saturation analysis of the multidate ERS-1 data also revealed improved wetland discrimination, particularly in combination with Indian Remote Sensing Satellite (IRSS) sensor data when compared to SAR-only data. In addition, C-band SAR imagery have been applied to mapping forested wetlands, a challenging vegetation assemblage for multispectral or single-source remote sensing imagery. In their multitemporal analysis of ERS-2, ENVISAT ASAR, and Landsat Enhanced Thematic Mapper Plus (ETM+), Lang et al. (2008) were able to demonstrate success of empirical Principal Components Analysis (PCA) to delineate hydroperiod-related classes of forested wetlands in the Mid-Atlantic, USA. Time series remote sensing and change detection are also exploiting seasonal, interannual, and phenologic changes in surfaces (Lunetta and Elvidge, 1998.) Multisensor SAR imagery over a period of twelve years was also able to detect coastal wetland shoreline change using edge-detecting filters with JERS-1 and Advanced Land Observation Satellite (ALOS) Phased-Array L-band SAR (PALSAR) imagery in the Pamlico Sound, North Carolina (Wang and Allen, 2008.)

Remote sensing, field, and environmental modeling data stored and analyzed within Geographic Information Systems (GIS) have played a strong and increasing role wetland mapping, such as the provision of floodplain boundaries and frequency of inundation simulations (Coe 2000.) Hydrogeomorphic conditions dominate the environmental gradients of riverine and coastal wetlands, affecting their biodiversity patterns (Hupp 1988) and zonation that can be discerned via remote sensing and environmental simulations of hydrology. Digital shoreline data, mapped via field, boat, or aerial imagery sources, is frequently used to mask aquatic and terrestrial zones for simplification of coastal remote sensing problems. Multisensor data can also be valuable, such as the utilization of imagery with infra-red reflectance data to rapidly map shorelines and develop mask layers for land-water separation. In addition, Light Detection and Ranging (LiDAR) has emerged as a revolutionary data source for mapping dynamic landforms and water levels (Hofle et al. 2009.) As the multitude of potential remote sensing data sources, algorithms, and classifications grows, it is prudent to expose potential methods and products to scrutiny and rigorous accuracy assessment. Several comprehensive past and ongoing remote sensing products have demonstrated useful insights from well-thought feasibility, prototyping, and accuracy assessments, including the NOAA Coastal Change Analysis Program (C-CAP) (Jensen et al., 1993), CoastWatch (Dobson and Bright, 1991; Klemas 1993), and USGS North American Landscape Characterization (NALC) archive (Loveland et al., 2000.)

Objectives. Our project aimed to assess the feasibility and achievable accuracy for multidate Synthetic Aperture Radar (SAR) and integrated RS-GIS data to classify coastal wetlands with high thematic and spatial resolution analogous to the US Fish and Wildlife Service's National Wetland Inventory (NWI) in a pilot study area of coastal North Carolina. We specifically intend to reveal the capability and accuracy of ALOS PALSAR and LiDAR input data combinations (e.g., SAR-only, combined SAR and LiDAR, and permutations of derivative LiDAR minimum elevation, vegetation canopy height, and slope.) Target thematic classes include palustrine forested wetlands

(pocosins, swamp forests, and pond pine forested shrubland), shrub-scrub wetland thickets, estuarine emergent wetlands (salt and brackish marshes), and patches of invasive *Phragmites australis* shores routinely establishing on the estuarine fringe of the Pamlico Sound.

METHODS

Study Area

The selected study area for this pilot project (Figure 1.) includes the coastal marshes of the US Fish and Wildlife (FWS) Alligator River National Wildlife Refuge (ARNWR), located along the shore of the Croatan and Pamlico Sounds in eastern North Carolina. The remote site exhibits few vehicular passable roads and extensive mosaics of pocosin and swamp forests, shrub-scrub, and emergent brackish and salt marshes, as well as sporadic patches of *Phragmites*. The region is representative of low-lying coastal plain swamp and marshlands, including the situation of the micro-tidal inundation regime dominated by infrequent wind tides. Thick peat soils and deep artificial ditches pose logistical limits on cropland, forestry, and human settlements. The study area is approximately 20Km north-south and 10Km wide east-west along the Croatan-Pamlico Sounds on the eastern shore of the



Figure 1. Study area location, Alligator River National Wildlife Refuge, North Carolina.

Pamlico Peninsula. The area was also selected owing to availability of prior FWS NWI mapping (ca. 1983) and ongoing updates in spring and summer 2010. The area would serve as the first of two areas selected, initially this site for methodology development, accuracy assessment and calibration. Subsequently, a second phase of analysis on performance and criticality of product and results will be undertaken and reported later for sites in Swan Quarter and/or Cedar Island National Wildlife Refuges.

Data Acquisition and Preprocessing

The study searched the data holdings of the Japanese Aerospace Exploration Agency (JAXA) and Alaska Satellite Facility (the relevant ground receiving station for the region) to procure a time series of ALOS PALSAR imagery. Three scenes were identified and acquired for 2010 images of PALSAR L-band HH and HV polarization SAR: 1) 40 April 2010, 2) 15 June 2010, and 3) 15 September 2010. This year coincided with near-normal precipitation and temperature regimes during the spring-summer seasons. In addition, LiDAR data were acquired for the area from the N.C. Floodplain Mapping Program for 2002, and digital aerial orthophotography was obtained from March-April 2010 for the area from the NC repository of the US Department of Agriculture National Agricultural Imagery Program (NAIP) (true-color composites.) PALSAR data were checked for georectification accuracy against the NAIP imagery and LiDAR, and each image was converted from digital number

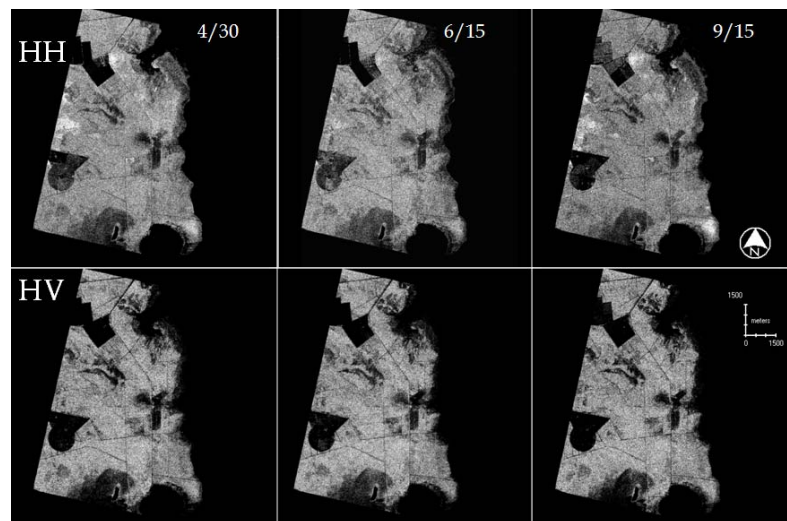


Figure 2. PALSAR multistatic images April, June, and September 2010.

(DN) into radar backscatter coefficient (measured in dB) as reported by Wang and Allen (2008.) All data were reprojected and resampled with nearest-neighbor analysis to Universal Transverse Mercator-194 (WGS84) for common earth coordinate system. Non-adapted speckle filters were applied to reduce noise in the PALSAR data, ultimately with selection of a 3x3 median filter in order to preserve step edges and ecotones between potential vegetation zones. This technique would reduce isolated pulses and yet provide a systematic method for subsequent analysis in other areas without the need to adjust adaptive filter weights (Tso and Mather, 2001.) LiDAR data included previously developed digital surface

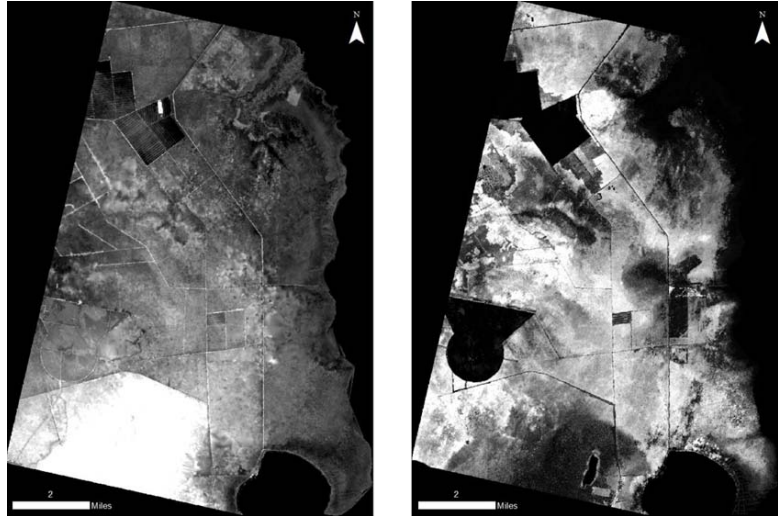


Figure 3. LiDAR derived (a) DEM and (b) vegetation canopy height.

models, resampled to 3m resolution digital elevation models (DEMs.) In addition, while last-return LiDAR points were developed for the bare earth DEM used in floodplain mapping and hydrologic modeling, we also acquired a vegetation canopy height DEM based on the first-return LiDAR points (D. Newcomb, personal communication.) Slope, profile, and planform curvature were derived for the bare earth DEM as potential input layers for classification using ArcGIS10 and GRASS GIS. A master raster database was constructed with potential inputs for image classification: 1-6) SAR HH and HV backscatter coefficients for the three image dates (Figure 2); 7) bare earth LiDAR-derived DEM; 8) slope; 9-10) DEM planform and profile curvature; and 11) LiDAR first-return vegetation canopy height surface. LiDAR bare earth DEM and vegetation canopy height are illustrated in Figure 3 (a and b, respectively.) The range of elevations is 0-6m, while vegetation canopy ranges 0-20m.

Image Classification

Our method for image classification subdivided the image subset into four combinations of data: 1) SAR-only, including HH and HV bands; 2) SAR plus LiDAR DEM; 3) SAR with canopy height; and SAR with DEM and canopy height. Preliminary analysis of the slope and curvature images resulted in gross errors, a result of the limited topographic relief for the area (most slopes < 1 degree and only isolated, rare instances of measureable slope curvature.) We employed ISODATA unsupervised classification as a first order technique for evaluating potential discernibility among key vegetation classes including, palustrine forest, shrub-scrub, estuarine emergent marshes, and *Phragmites*. We also evaluated variable number of clusters (10, 15, and 20), and convergence thresholds, and the adoption of a water mask (precluding open water from entering the classification.) One image analyst conducted each of the image classifications, utilizing the 2010 provisional NWI aerial photointerpreted vegetation map as a guide, along with ground photos and field expert knowledge. A separate image analyst conducted the accuracy assessment, utilizing NAIP imagery and field observations and expertise of an on-site ecologist.

Accuracy Assessment

Accuracy assessment sought to evaluate a variety of quality characteristics of the produced maps, including Producer's, User's, and overall accuracy, as well as deriving the Kappa (K-hat) coefficient as a comparative statistic to other potential classification techniques and products. Owing to the inaccessibility and potential to require ground-based observational verification, we subdivided the classified images into three intensive study areas (ISAs), centered on Spencer Creek (an estuarine creek to the north, fronting Croatan Sound), Point Peter Road (site of an ecological restoration project by The Nature Conservancy, and one of the few roads transecting most vegetation units), and Stumpy Point (a community in the south of the area, fronting Pamlico Sound, with several points of vehicular and foot transit.) For each image, 300 test points were sampled in a stratified random technique utilizing a 3x3 majority threshold for pixel selection ($Threshold=7$). This potentially positively biased criterion was sought to mitigate errors that might be imparted from the variable spatial positional accuracy of both reference verification data and input SAR and DEM data. 2010 NWI maps, 2010 color orthophotography, and field observations were utilized to label test pixel reference values while the classified categories were blind to the analyst. Error matrices, accuracy percentages, and overall accuracy and Kappa statistics were generated for each attempt.

RESULTS AND DISCUSSION

Results of the image classification are shown in map form in Figure 4 a-d, depicting the overall mosaic of classes. The SAR-only classification (4a) performed exceptionally well qualitatively with respect to marsh, shrub-scrub, and palustrine forest extent and pattern (overall Kappa 0.742). The SAR-only classification yielded an overall accuracy of 80.7% with relatively high user's accuracy by class (lowest for water with 63.3% while vegetation ranged 71.9% for shrub-scrub to 89.7% for marshes.) The SAR and DEM classification (4b) identified an overabundance of *Phragmites*, particularly in the Spencer Creek north area (overall Kappa 0.52). The SAR+DEM combination suffered low accuracy with *Phragmites* (user's accuracy 42.8%) and marshes (54.4%), likely as a fundamental result of low-lying fringe vegetation being indeterminate for interpolated bare earth LiDAR points. SAR and canopy height classification (4c) is visually good, with moderate error in overestimating the extent of *Phragmites* and open water within Spencer Creek (Kappa = 0.726). SAR+canopy height classified data was superior to SAR+DEM, with better *Phragmites* results (user's accuracy 61.1%) and much improved shrub-scrub accuracy (72.8%). Finally, the SAR imagery with DEM and canopy height included resulted in a good overall upland classification and modest error, visually, among the water and *Phragmites*. This image (4d) nonetheless identified forest and shrub-scrub discernment very well (Kappa overall 0.744). The overall accuracy for this composite classification using SAR, DEM, and vegetation canopy height was 81.33%, with a surprising disappointment with confusion of water (60% user's accuracy). This result is nonetheless very promising, as incorporating a more robust shoreline water mask or infrared-based spectral mask would dramatically reduce this source of confusion (found mainly with commission errors, water being classified as *Phragmites*.) However, it is equally possible that *Phragmites* is so dynamic in this area, that is *in truth* was present at the time imagery was collected. Our field visit with FWS staff and on-site ecologists from The Nature Conservancy (TNC) revealed that the some large areas of *Phragmites* had just been sprayed by aerial application of herbicides. As a result, the interpretation that open water was *not* this type vegetation could be in error. Other vegetation was not sprayed, buoying our inference that this initial methodology and combination of data sources could provide a robust and effective method for coastal wetland mapping.

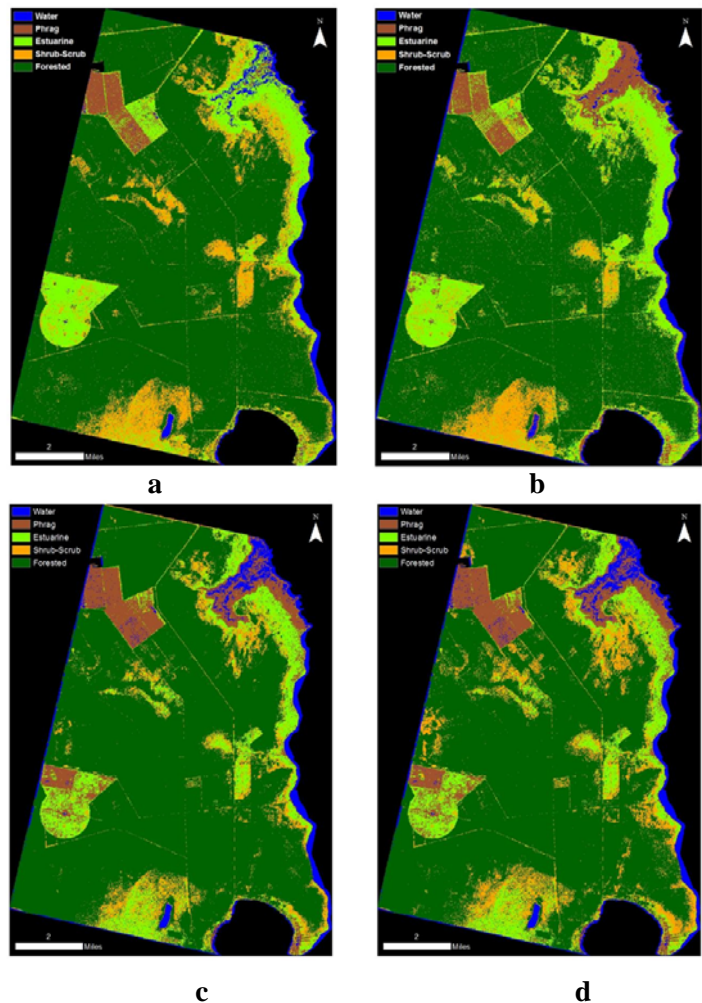


Figure 4. Results of four image classifications a) SAR-only, b) SAR with DEM, c) SAR with canopy height, and d) SAR with DEM and canopy height.

CONCLUSIONS

Although results reported in this project are preliminary, we suggest that the literature and convergence of SAR, LiDAR, and geospatial analysis is now mature to the point that heretofore methods for regional wetland inventorying and mapping are highly promising. This project has shown that good accuracy and even high user's

accuracy can be generated from the combination of multitemporal SAR and LiDAR. The relatively good accuracy and inexpensive source imagery (ALOS PALSAR) should spur future such missions for coastal mapping, and the application of LiDAR beyond its original floodplain mapping purposes illustrates a strong value-addition to coastal resource and environmental managers. A surprising and further promising result was the relatively good accuracy achieved for *Phragmites* class, particularly in the SAR-only time series classification (85.7% user's accuracy.) Conservatively, however, the second phase of this research remains to be undertaken, the best data combinations and classification algorithms will be applied to a second test area as an evaluation of the portability and robustness of the approach.

REFERENCES

- Borgeau-Chavez, L.L., K.B. Smith, S.M., Brunzell, E.S. Kasischke, E.A. Romanowicz, and C.J. Richardson, 2005. Remote sensing of regional inundation patterns and hydroperiod in the Greater Everglades using synthetic aperture radar. *Wetlands*, 25(1):176-191.
- Coe, M.T., 2000. Modeling terrestrial hydrologic systems at the continental scale: Testing the accuracy of an atmospheric GCM. *Journal of Climate*, 13:686-704.
- Dobson, J.D. and E.A. Bright, 1991. CoastWatch- Detecting Change in Coastal Wetlands. *Geo Info Systems*, January, 36-40.
- Franklin, S.E., 1991. Satellite remote sensing of mountain geomorphic surfaces, *Canadian Journal of Remote Sensing*, 17(3):218-229.
- Hamilton, S.K., J. Kellendorfer, B. Lehner, and M. Tobler, 2007. Remote sensing of floodplain geomorphology as a surrogate for biodiversity in a tropical river system (Madre de Dios, Peru.), *Geomorphology*, 89:23-38.
- Hofle, B., M. Vetter, N. Pfeiffer, G. Mandlbürger, and J. Stotter, 2009. Water surface mapping from airborne laser scanning using signal intensity and elevation data. *Earth Surface Processes and Landforms*, 34(12):1635-1649.
- Hupp, C.R., 1988. Plant ecological aspects of flood geomorphology and paleoflood history. In: Baker, V.R., Kochel, C.R., Patton, R.C. (Eds.), *Flood Geomorphology*, Wiley, pp. 335-356.
- Jensen, J.R., D. Cowen, J.D. Althausen, S. Narumalani, and O. Weatherbee. 1993. An evaluation of CoastWatch change detection protocol in South Carolina. *Photogrammetric Engineering and Remote Sensing*, 59(6): 1039-1046.
- Kasischke, E.L. and L.L. Borgeau-Chavez. 1997. Monitoring south Florida wetlands using ERS-1 SAR imagery. *Photogrammetry and Remote Sensing*, 63:281-291.
- Klemas, V.V., J.E. Dobson, R.L. Ferguson, and K.D. Haddad. 1993. A coastal land cover classification system for the NOAA Coastwatch Change Analysis Project. *Journal of Coastal Research*, 9(3): 862-872
- Kushwaha, S.P.S., R.S. Dwivedi, and B.R.M. Rao. 2000. Evaluation of various digital image processing techniques for detection of coastal wetlands using ERS-1 SAR data. *International Journal of Remote Sensing*, 21(3):565-579.
- Lang, M.W., E.S. Kasischke, S.D. Prince, and K.W. Pittman. 2008. Assessment of C-band synthetic aperture radar for mapping and monitoring Coastal Plain forested wetlands in the Mid-Atlantic Region, U.S.A., *Remote Sensing of Environment*, 112:4120-4130.
- Loveland, T.R., Merchant, J.W., Ohlen, D.O. and Brown, J.F., 1991. Development of a land-cover characteristics database for the conterminous U.S. *Photogrammetric Engineering and Remote Sensing*, 57(11):1453-1463.
- Lunetta, R.S. and C.D. Elvidge. 1998. Eds., *Remote Sensing Change Detection: Environmental Monitoring Methods and Applications*, Taylor and Francis, London, 318 p.
- Tso, B. and P.M. Mather, 2001. *Classification Methods for Remotely Sensed Data*, Taylor and Francis, London, 332 pp.